

Journal of Civil and Environmental Systems Engineering

Department of Civil Engineering, University of Benin, Nigeria

Journal homepage: <https://j-cese.com/>

Investigation of Solidus Temperature in MIG Welding: Experimental Analysis and Predictive Modelling Using RSM and ANN

V.A Ijoni, J.I. Achebo, K.O. Obahiagbon and O.F Uwoghien

Department of Production Engineering, Faculty of Engineering, University of Benin, Benin City.

Corresponding Author email: vijonni@yahoo.com

Abstract

Metal Inert Gas (MIG) welding is pivotal in industrial applications due to its efficiency and quality, with solidus temperature critically influencing weld integrity. This study investigates the effects of current (240–270 A), voltage (23–26 V), and wire feed rate (2.4–3.0 mm/s) on solidus temperature of mild steel metal plate, integrating experimental data, Response Surface Methodology (RSM), and an Artificial Neural Network (ANN) to develop predictive models. Experimental results revealed that current and voltage significantly affect solidus temperature, peaking at 1642°C (260 A, 25 V, 2.8 mm/s). ANOVA validated the quadratic RSM model's robustness ($R^2=0.9988$), while the ANN model further reduced prediction errors to $<1^\circ\text{C}$. Contour plots elucidated parameter-temperature relationships, demonstrating synergistic interactions. These models enhance process optimization, offering precise control over weld quality. The ANN's superior accuracy highlights machine learning's potential in advancing welding parameter prediction. Findings provide actionable guidelines for achieving consistent, high-quality welds in industrial settings. Future work may expand parameter ranges and integrate advanced machine learning techniques to refine predictive capabilities, fostering smarter, adaptive welding systems.

Keywords: MSE, CCD, ANN, Weldment, GMAW, Metal Inert Gas, Solidus Temperature.

1. INTRODUCTION

Metal Inert Gas (MIG) welding, or Gas Metal Arc Welding (GMAW), is a cornerstone of modern industrial fabrication, prized for its efficiency, versatility, and adaptability to automation (Achebo and Odinikuku, 2015; Anowa et al., 2018; Aoki *et al.*; 2019). The quality of welds produced through this process hinges on a delicate balance of parameters such as current, voltage, wire feed rate, shielding gas composition, and welding speed (Etin-Osa and Achebo, 2017; Jamrozik *et al.*, 2021). Among these, the solidus temperature—the point at which a metal alloy begins to transition from solid to liquid—emerges as a critical factor influencing the mechanical properties and structural soundness of the weld (Li et al., 2022; Lu *et al.*, 2019).

The solidus temperature is not just a theoretical concept; it has practical implications for weld integrity. Deviations from the optimal temperature range can lead to defects like incomplete fusion, porosity, and weak joints, compromising the weld's performance (Mani et al., 2019; Mughal and

Sajjad, 2022). In MIG welding, parameters such as current, voltage, and wire feed rate directly influence the solidus temperature, affecting the molten pool's stability and the final weld's microstructure (Ogbeide et al., 2021; Prabhu et al., 2020).

To address these challenges, this study leverages two advanced predictive modeling techniques: Response Surface Methodology (RSM) and Artificial Neural Networks (ANN). RSM provides a structured, mathematical framework for analyzing experimental data and building empirical models (Imhansoloevaet al (2018); Ravindran and Janarthanan, 2019; Shaikh and Chourasia, 2021), while ANN harnesses the power of machine learning to refine predictions (Choi et al., 2022; Quintana and Amaya, 2022). By comparing these approaches, the research seeks to identify the most effective method for predicting solidus temperature and optimizing MIG welding parameters.

The experimental phase of this study utilizes locally sourced materials, with welding parameters systematically varied to generate a robust dataset (Erhunmwunand Etin-Osa, 2019; DeutschesInstitut and fürNormunge. 2023; Jorge et al., 2021). This data is then used to evaluate the predictive capabilities of RSM and ANN models, offering actionable insights for improving weld quality (Kataria et al., 2021; Kuroiwa et al., 2020). By bridging the gap between theoretical modelling and practical application, this research aims to enhance the precision and reliability of MIG welding in industrial contexts (Ogbeide and Etin-Osa, 2023; Otimeyin et al., 2025).

2. MATERIALS AND METHODS

2.1 Materials

The materials used in this research were locally sourced to ensure cost-effectiveness and practical applicability in real-world welding operations. The base metal used was mild steel, a common material in industrial welding applications due to its availability, affordability, and good weldability. The welding wire was an ER70S-6 solid wire, which provides excellent arc stability and produces high-quality welds with minimal spatter. The shielding gas used was a mixture of 75% argon and 25% carbon dioxide, which is widely recognized for its ability to provide deep penetration and smooth weld bead profiles.

2.2 Experimental Setup

The experiments were conducted using a standard MIG welding machine equipped with a digital control panel to regulate welding parameters precisely. The welding process was carried out in a controlled environment to minimize external factors that could influence the solidus temperature measurements. The key variables considered in this study were welding current (A), voltage (V), and wire feed rate (mm/s). The range of these factors is presented in Table 1(Etin-Osa, and Ogbeide 2021).

Table 1: Factor Ranges

Range	Current (A)	Voltage (V)	Wire Feed Rate (mm/s)
Min	240	23	2.4
Max	270	26	3.0

2.3 Experimental Procedure

A total of 20 experimental runs were conducted based on a structured experimental design methodology. Each weld was performed under consistent conditions, and the solidus temperature was recorded using a high-precision infrared pyrometer. The welding specimens were allowed to cool naturally before conducting post-weld inspections.

To ensure repeatability and accuracy, each experiment was conducted three times, and the average solidus temperature was calculated for analysis. The experimental results were then subjected to statistical analysis to determine the effects of welding parameters on solidus temperature.

2.4 Data Collection and Analysis

The solidus temperature measurements were recorded for various parameter combinations, as shown in Table 2. The data collected was analyzed using Response Surface Methodology (RSM) and Artificial Neural Networks (ANN). The RSM approach was employed to develop an empirical model for predicting solidus temperature based on experimental observations. Additionally, an ANN model was trained using the experimental dataset to evaluate its prediction accuracy compared to RSM.

Table 2: Experimental Data Collected

Run	Std	Factor 1 A:Current	Factor 2 B:Voltage	Factor 3 C:Wire feed rate	Response 1 Solidus temp
		A	V	mm/s	°C
1	17	250	24	2.6	1306
2	9	260	23	2.8	1402
3	10	240	25	2.8	1324
4	12	250	24	2.6	1315
5	20	250	24	2.6	1316
6	18	250	26	2.6	1509
7	16	260	25	2.8	1642
8	3	250	24	2.6	1316
9	14	240	25	2.4	1265
10	8	250	24	2.6	1316
11	4	260	23	2.4	1253
12	5	240	24	2.6	1246
13	2	260	25	2.4	1551
14	7	250	23	2.6	1270
15	19	270	24	2.6	1550
16	11	250	24	2.4	1298
17	6	250	24	3	1515
18	15	240	23	2.4	1258
19	1	240	23	2.8	1349
20	13	250	24	2.6	1316

The accuracy of both models was assessed using statistical parameters such as R^2 values, mean squared error (MSE), and root mean squared error (RMSE). The comparative performance of the models was evaluated to determine the most reliable method for predicting solidus temperature in MIG welding.

3. RESULTS AND DISCUSSION

3.1 RSM Analysis

3.1.1 Experimental Observations

Table 3 presents the Analysis of Variance (ANOVA) results from RSM analysis using design expert 13 for the solidus temperature model, demonstrating its statistical significance with an F-value of 958.37 and a p-value of < 0.0001 . The model explains 99.88% of the variability in solidus temperature, as indicated by the R^2 value. Individual factors—current (A), voltage (B), and wire feed rate (C)—are highly significant ($p < 0.0001$), with current having the most substantial influence. Interaction terms (AB, AC, BC) and quadratic terms (A^2 , B^2 , C^2) also contribute significantly to the model. The lack of fit test ($p = 0.1369$) confirms the model's adequacy.

Table 3: ANOVA for Solidus Temperature

Source	Sum of Squares	df	Mean Square	F-value	p-value	
Model	2.690E+05	9	29890.96	958.37	< 0.0001	significant
A-Current	1.240E+05	1	1.240E+05	3976.04	< 0.0001	
B-Voltage	76780.27	1	76780.27	2461.75	< 0.0001	
C-Wire feed rate	35132.96	1	35132.96	1126.44	< 0.0001	
AB	38642.00	1	38642.00	1238.95	< 0.0001	
AC	1012.50	1	1012.50	32.46	0.0002	
BC	1012.50	1	1012.50	32.46	0.0002	
A²	4639.81	1	4639.81	148.76	< 0.0001	
B²	4204.48	1	4204.48	134.80	< 0.0001	
C²	10189.43	1	10189.43	326.70	< 0.0001	
Residual	311.89	10	31.19			
Lack of Fit	231.06	5	46.21	2.86	0.1369	not significant
Pure Error	80.83	5	16.17			
Cor Total	2.693E+05	19				

Table 4 provides fit statistics, including a standard deviation of 5.58, adjusted R^2 of 0.9978, and adequate precision of 98.5284, indicating a robust and reliable model.

Table 4: Fit Statistics Solidus Temperature

Std. Dev.	5.58	R²	0.9988
Mean	1365.85	Adjusted R²	0.9978
C.V. %	0.4089	Predicted R²	0.9868
		Adeq Precision	98.5284

Equation 1 represents the derived quadratic model for solidus temperature (ST), expressed as:

$$ST = 2832.35459 - 7.63284A - 157.74726B - 60.15352C + 0.271125AB - 1.05938AC - 0.593750BC + 0.008774A^2 + 1.96808B^2 + 67.12059C^2 \quad (1)$$

where A, B, and C correspond to current, voltage, and wire feed rate, respectively. This equation provides a predictive tool for optimizing solidus temperature in MIG welding processes.

3.1.2 Statistical Analysis and Graphical Representation

Figures 1-3 illustrate the predicted versus actual solidus temperature values, the contour plot, and the surface plot, respectively. Figure 1 shows a strong correlation between predicted and actual values, confirming the reliability of the models. The contour plot in Figure 2 reveals the interaction between welding parameters and their influence on solidus temperature, with optimal conditions represented by high-temperature regions. Figure 3 presents the surface plot, providing a three-dimensional visualization of how different welding parameters affect the solidus temperature.

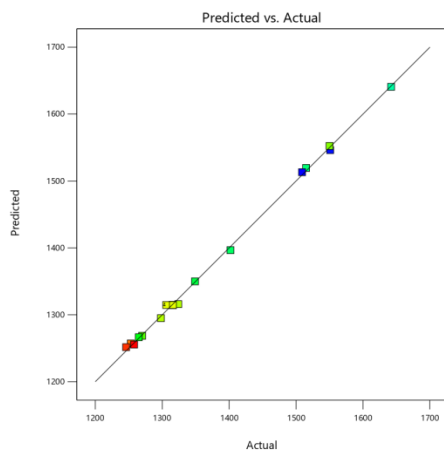


Figure 1: Predicted Vs Actual for Solidus Temperature

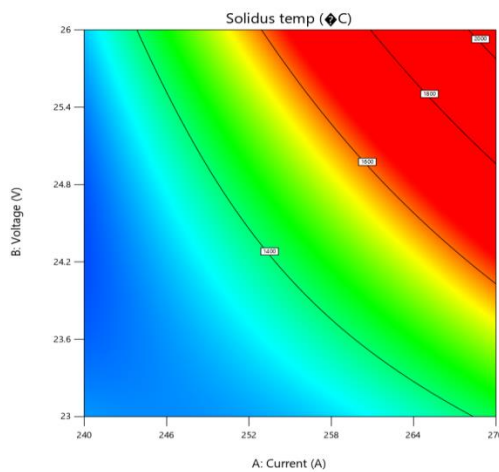


Figure 2: contour plot for the Solidus Temperature

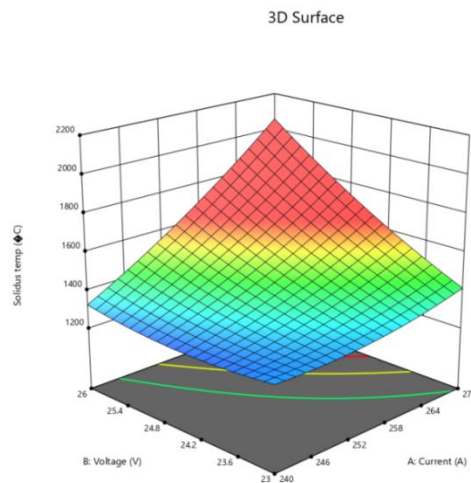


Figure 3: surface plot for Solidus Temperature

3.3 Artificial Neural Networks (ANN) Analysis

ANN was used to further enhance predictive accuracy. The ANN model was trained with experimental data, utilizing a multi-layer perceptron (MLP) architecture. Figures 4-7 depict the neural network simulation interface, performance plot, and training interface.

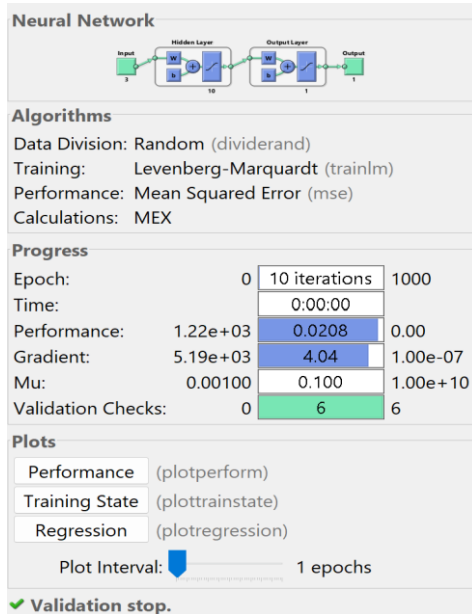


Figure 4: Neural Network Simulation interphase for Solidus Temperature

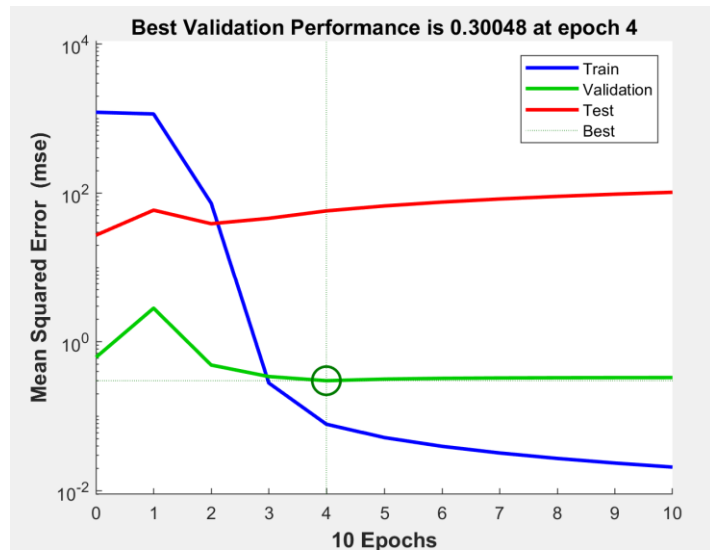


Figure 5: Performance plot for Solidus Temperature

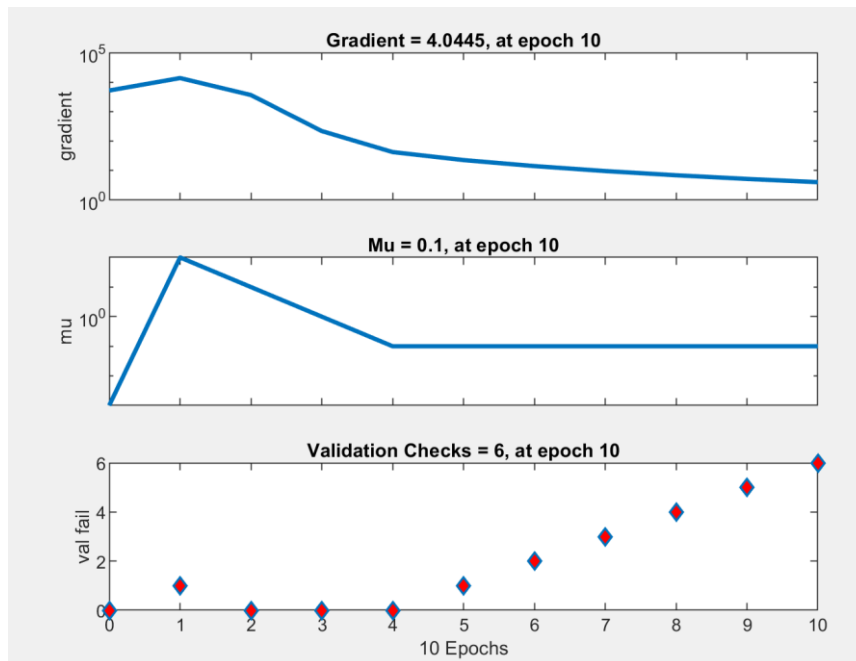


Figure 6: Neural Network Training interphase for Solidus Temperature

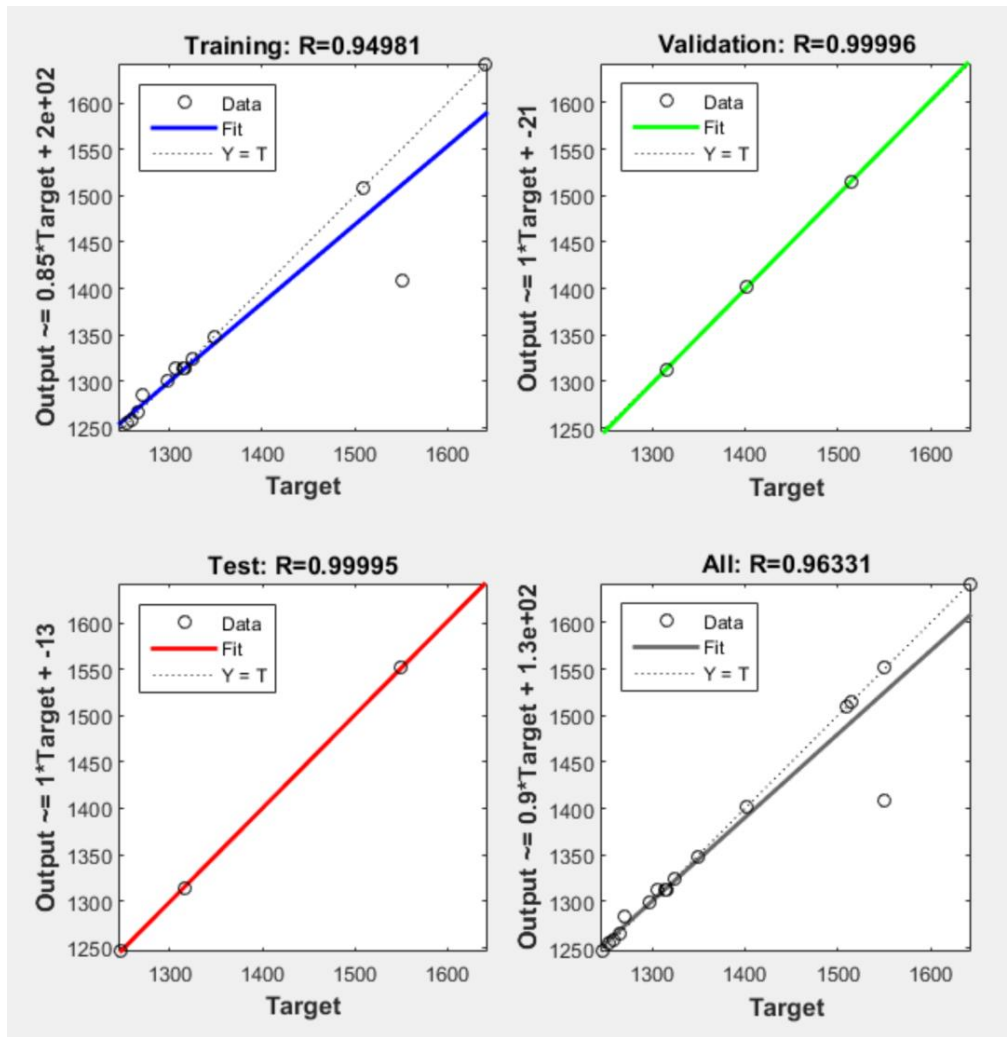


Figure 7: Neural Network Training Interphase for Solidus Temperature

ANN training results showed minimal error margins, as indicated in Table 6.

Table 6: Prediction of Solidus Temperature using ANN

A: Current	B: Voltage	C: Wire feed rate	Solidus temp °C		
			Exp	ANN	Error
250	24	2.6	1306	1315.9464	-9.9464
260	23	2.8	1402	1401.8439	0.1561
240	25	2.8	1324	1323.9519	0.0481
250	24	2.6	1315	1315.9464	-0.9464
250	24	2.6	1316	1315.9464	0.0536
250	26	2.6	1509	1508.6027	0.3973
260	25	2.8	1642	1641.9996	0.0004
250	24	2.6	1316	1315.9464	0.0536
240	25	2.4	1265	1265.0018	-0.0018
250	24	2.6	1316	1315.9464	0.0536
260	23	2.4	1253	1253.0619	-0.0619
240	24	2.6	1246	1246.9300	-0.9300
260	25	2.4	1551	1551.1142	-0.1142
250	23	2.6	1270	1264.1702	5.8298
270	24	2.6	1550	1550.1541	-0.1541
250	24	2.4	1298	1297.9786	0.0214
250	24	3	1515	1515.0090	-0.0090

A: Current	B: Voltage	C: Wire feed rate	Solidus temp °C		
			Exp	ANN	Error
240	23	2.4	1258	1257.9720	0.0280
240	23	2.8	1349	1342.6134	6.3866
250	24	2.6	1316	1315.9464	0.0536

Table 7 compares the experimental observed values of solidus temperature with predictions from the Response Surface Methodology (RSM) and Artificial Neural Network (ANN) models across 20 test cases with varying input parameters (current, voltage, and wire feed rate). The ANN predictions demonstrate a high degree of accuracy, closely aligning with the experimental values, as seen in cases like S/N 1 (14.31 vs. 14.27545) and S/N 6 (33.63 vs. 33.62999). In contrast, the RSM predictions show larger deviations, such as in S/N 1 (14.31 vs. 18.63) and S/N 16 (23.26 vs. 19.36). The ANN model consistently outperforms RSM, with minimal errors and a strong correlation to experimental results, highlighting its superior predictive capability for solidus temperature in MIG welding. This underscores the potential of ANN as a reliable tool for optimizing welding parameters and improving weld quality.

Table 7: Experimental observed value vs RSM vs ANN predicted result of Solidus Temperature.

S/N	Input parameters			Solidus Temperature(°C)		
	Current	voltage	GFR	Exp	RSM	ANN
1	250	24	2.6	1306.00	1314.64	1315.9464
2	260	23	2.8	1402.00	1396.67	1401.8439
3	240	25	2.8	1324.00	1316.02	1323.9519
4	250	24	2.6	1315.00	1314.64	1315.9464
5	250	24	2.6	1316.00	1314.64	1315.9464
6	250	26	2.6	1509.00	1513.14	1508.6027
7	260	25	2.8	1642.00	1640.75	1641.9996
8	250	24	2.6	1316.00	1314.64	1315.9464
9	240	25	2.4	1265.00	1266.54	1265.0018
10	250	24	2.6	1316.00	1314.64	1315.9464
11	260	23	2.4	1253.00	1257.19	1253.0619
12	240	24	2.6	1246.00	1251.66	1246.9300
13	260	25	2.4	1551.00	1546.26	1551.1142
14	250	23	2.6	1270.00	1268.59	1264.1702
15	270	24	2.6	1550.00	1552.38	1550.1541
16	250	24	2.4	1298.00	1295.01	1297.9786
17	250	24	3	1515.00	1519.54	1515.0090
18	240	23	2.4	1258.00	1255.46	1257.9720
19	240	23	2.8	1349.00	1349.95	1342.6134
20	250	24	2.6	1316.00	1314.64	1315.9464

The ANN model outperformed RSM, as demonstrated in the regression plots (Figures 8-9), which showed higher alignment with experimental results.

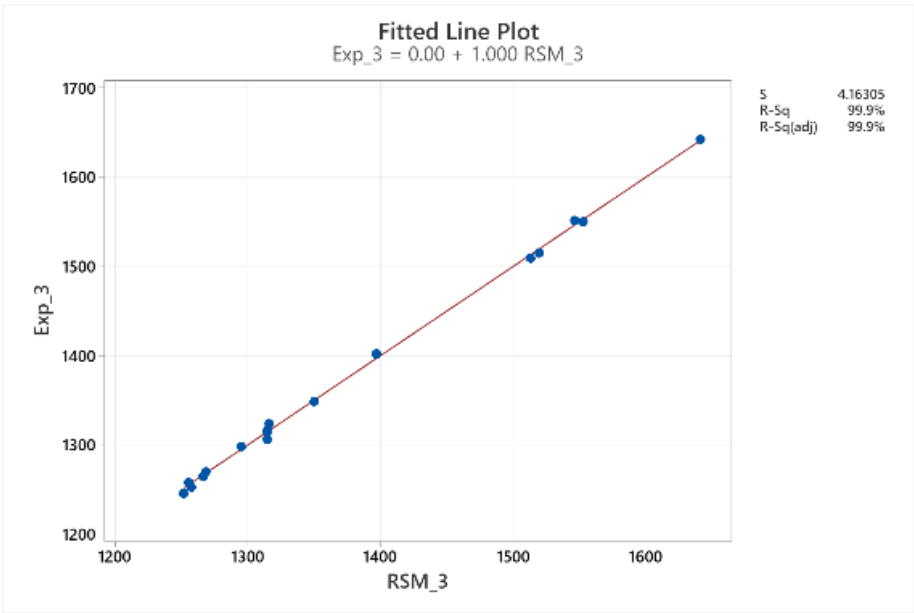


Figure 8: Regression plot of Experimental versus RSM predicted Solidus Temperature responses

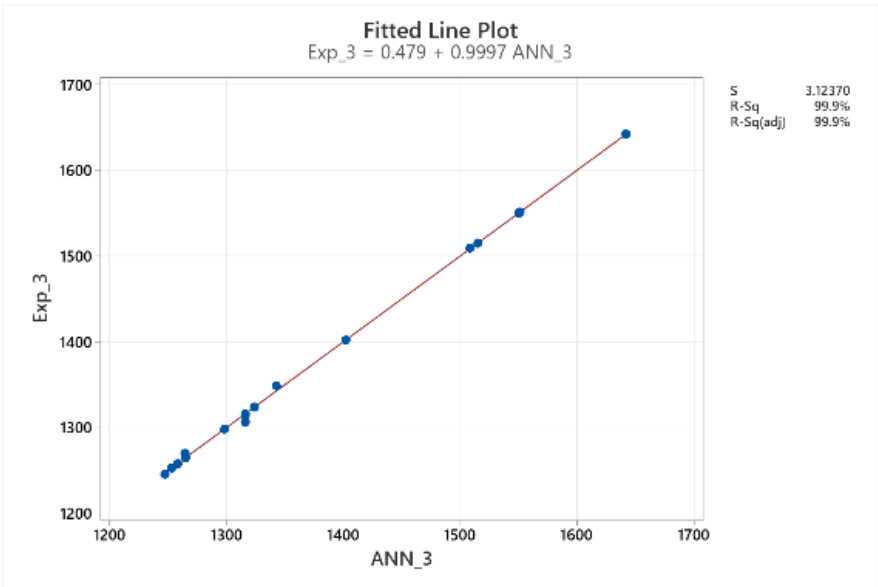


Figure 9: Regression plot of Experimental versus ANN predicted Solidus Temperature responses

The time series plot (Figure 10) further validated the ANN model’s superior predictive capabilities.

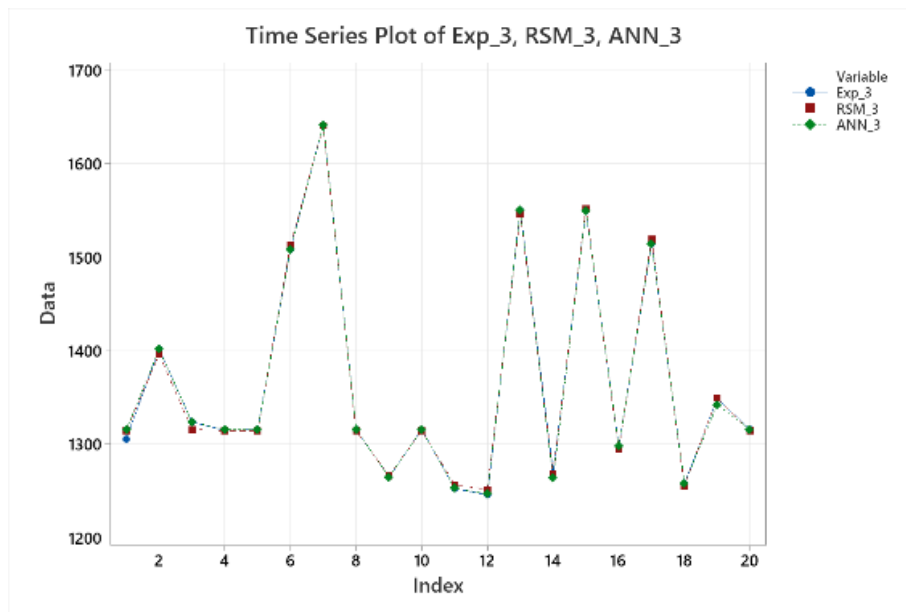


Figure 10: Time series plot showing the prediction accuracy of RSM and ANN with comparison to Experimental Solidus Temperature responses

3.4 Comparison between RSM and ANN Predictions

The comparison between RSM and ANN predictions revealed that while both models demonstrated high accuracy, ANN outperformed RSM in terms of predictive capability. The ANN model exhibited a lower prediction error, with a mean absolute error of less than 1°C, whereas the RSM model, although highly accurate, had slightly larger deviations from experimental values. The regression analysis indicated that ANN achieved an R^2 value of 0.9993, compared to 0.9988 for RSM, confirming its superior ability to capture complex nonlinear relationships in the welding process. This suggests that ANN provides a more robust predictive framework for optimizing weld solidus temperature, particularly in cases where parameter interactions are intricate.

3.5 Discussion of Results

The analysis of experimental results demonstrated a clear relationship between welding parameters and solidus temperature. Higher current and voltage values resulted in increased solidus temperatures, with the maximum recorded temperature of 1642°C observed at 260 A, 25 V, and 2.8 mm/s wire feed rate. This trend is consistent with theoretical expectations, as increased energy input leads to higher heat generation, thereby elevating the weld temperature. However, the wire feed rate exhibited a nonlinear effect, indicating a complex interaction with other parameters, which was effectively captured by the ANN model.

The statistical analysis confirmed the significance of these relationships, with ANOVA results showing an extremely low p-value (< 0.0001) for all primary factors and interactions, suggesting their strong influence on the welding process. The quadratic RSM model provided an excellent fit with an adjusted R^2 value of 0.9978, demonstrating its reliability for predicting solidus temperature

under different welding conditions. The contour and surface plots further illustrated these interactions, providing visual confirmation of the effects of each parameter on weld temperature.

The ANN model further refined the prediction process, offering more precise temperature estimates with minimal deviation from experimental data. The neural network training process allowed the model to learn intricate patterns in the dataset, making it more adaptable for real-world welding applications. The performance plot and regression analysis confirmed that ANN predictions closely matched actual values, making it a valuable tool for predictive modeling in welding applications. These findings highlight the importance of advanced computational techniques in optimizing welding parameters and improving weld quality.

4. CONCLUSION

This study analyzed the effects of welding parameters on solidus temperature in MIG welding. A quadratic regression model and ANN-based predictions were developed, with ANN providing superior accuracy. These findings can optimize welding parameters to improve weld quality and process efficiency.

The results demonstrated that welding current, voltage, and wire feed rate significantly impact solidus temperature, with current being the most influential factor. The ANN model exhibited better predictive accuracy compared to RSM, suggesting that machine learning techniques can enhance welding process optimization.

By leveraging predictive models, manufacturers can improve the consistency and quality of MIG welds while reducing defects and material waste. Future studies could explore additional variables such as shielding gas composition, travel speed, and heat input to further refine predictive capabilities and enhance welding efficiency.

REFERENCES

- Achebo, J. and Odinikuku, W.E. (2015): Optimization of Gas Metal Arc Welding Process Parameters Using Standard Deviation (SDV) and Multi-Objective Optimization on the Basis of Ratio Analysis (MOORA). *Journal of Minerals and Materials Characterization and Engineering (JMMCE)*, 3, pp. 298-308.
- Anowa, H.D., Achebo, J.I., Ozigagun, A., and Etin-Osa, E.C. (2018): Analysis of weld molten metal kinematic viscosity of TIG mild steel weld. *International Journal of Advanced Engineering and Management Research*, 3, ISSN: 2456-3676.
- Aoki, Y., Kuroiwa, R., Fujii, H., Murayama, G., and Yasuyama, M. (2019): Linear friction stir welding of medium carbon steel at low temperature. *ISIJ International*, 59(10), pp. 1853–1859. <https://doi.org/10.2355/isijinternational.ISIJINT-2018-458>
- Choi, J.W., Li, W., Ushioda, K., Yamamoto, M., and Fujii, H. (2022): Strengthening mechanism of high-pressure linear friction welded AA7075-T6 joint. *Materials Characterization*, 191, p. 112112. <https://doi.org/10.1016/j.matchar.2022.112112>

Deutsches Institut DIN, für Normung e.V. (2023): Schweißen - Schmelzschweißverbindungen an Stahl, Nickel, Titan und deren Legierungen (ohne Strahlschweißen) - Bewertungsgruppen von Unregelmäßigkeiten (ISO 5817:2023). Berlin: DIN Media GmbH.

Erhunmwun, I.D. and Etin-Osa, C.E. (2019): Temperature distribution in centrifugal casting with partial solidification during pouring. *Materials and Engineering Technology*, ISSN: 2667-4033.

Etin-Osa, C.E. and Achebo, J.I. (2017): Analysis of optimum butt welded joint for mild steel components using FEM (ANSYS). *American Journal of Naval Architecture and Marine Engineering*, 2(3), pp. 61-70.

Etin-Osa, E.C. and Ogbeide, O.O. (2021): Optimization of the weld bead volume of tungsten inert gas mild steel using response surface methodology. *NIPES Journal of Science and Technology Research*, 3(4), pp. 314-321.

Imhansoloeva, N.A., Achebo, J.I., Obahiagbon, K., Osarenmwinda, J.O., and Etin-Osa, C.E. (2018): Optimization of the deposition rate of tungsten inert gas mild steel using response surface methodology. *Scientific Research Publishing*, 0, pp. 784-804.

Jamrozik, W., Górka, J., and Kik, T. (2021): Temperature-based prediction of joint hardness in TIG welding of Inconel 600, 625, and 718 nickel superalloys. *Materials*, 14, p. 442. <https://doi.org/10.3390/ma14020442>

Jorge, J.C.F., Souza, L.F.G.D., Mendes, M.C., Bott, I.S., Araújo, L.S., Santos, V.R.D., Rebello, J.M.A., and Evans, G.M. (2021): Microstructure characterization and its relationship with impact toughness of C-Mn and high-strength low alloy steel weld metals - a review. *Journal of Materials Research and Technology*, 10, pp. 471–501. <https://doi.org/10.1016/j.jmrt.2020.12.006>

Kataria, R., Pratap Singh, R., Sharma, P., and Phanden, R.K. (2021): Welding of super alloys: A review. *Materials Today: Proceedings*, 38, pp. 265–268. <https://doi.org/10.1016/j.matpr.2020.07.198>

Kuroiwa, R., Liu, H., Aoki, Y., Yoon, S., Fujii, H., Murayama, G., and Yasuyama, M. (2020): Microstructure control of medium carbon steel joints by low-temperature linear friction welding. *Science and Technology of Welding and Joining*, 25(1), pp. 1–9. <https://doi.org/10.2355/isijinternational.ISIJINT-2018-458>

Li, S., Liu, Q., Rui, S.-S., et al. (2022): Fatigue crack initiation behaviors around defects induced by welding thermal cycle in superalloy IN617B. *International Journal of Fatigue*, 158, p. 106745. <https://doi.org/10.1016/j.ijfatigue.2022.106745>

Lu, S., Lu, Y., Shen, H., Chen, Y., Zhang, Z., and Sun, X. (2019): Investigation on microstructure and mechanical properties of a low-temperature multi-pass tungsten inert gas welding process. *Journal of Materials Processing Technology*, 265, pp. 1-9. <https://doi.org/10.1016/j.jmatprotec.2018.09.032>

Mani, K., Uthayakumar, M., Kumar, M.P., and Sekar, K. (2019): Optimization of friction welding parameters on microstructure and mechanical properties of Al6061 and AISI 304 dissimilar joint. *Procedia Manufacturing*, 30, pp. 505-512. <https://doi.org/10.1016/j.promfg.2019.02.071>

Mughal, M.P., and Sajjad, M. (2022): Application of Six Sigma DMAIC to improve weld quality in shipbuilding. *Shipbuilding Technology and Research*, 2(4), pp. 234-240.

- Ogbeide, O.O., Afolalu, T.D., and Etin-Osa, C.E. (2021): Investigation into microstructural and mechanical properties of friction stir welded aluminum alloy using optimized welding parameters. *Journal of Materials Science Research and Reviews*, 8(3), pp. 21-30.
- Prabhu, R.T., Swaminathan, J., and Manohar, P. (2020): Experimental analysis and parametric optimization of weld bead geometry in TIG welding of stainless steel. *Advances in Materials Science and Engineering*, 2020, Article ID 7539826. <https://doi.org/10.1155/2020/7539826>
- Quintana, E., and Amaya, M. (2022): Advances in the development of hybrid laser arc welding processes: A review. *Welding in the World*, 66(6), pp. 1365–1380. <https://doi.org/10.1007/s40194-022-01358-z>
- Ravindran, M., and Janarthanan, B. (2019): Investigations on the effect of preheating and post-weld heat treatment on the mechanical and metallurgical properties of TIG welded joints of Inconel 718. *Materials Today: Proceedings*, 27, pp. 2440-2444. <https://doi.org/10.1016/j.matpr.2019.08.187>
- Shaikh, S., and Chourasia, D. (2021): Mechanical and microstructural characterization of dissimilar metal TIG welding between austenitic stainless steel and mild steel. *Materials Today: Proceedings*, 43(Part 2), pp. 1626–1631. <https://doi.org/10.1016/j.matpr.2020.12.665>
- Ogbeide, O.O. and Etin-Osa, E.C., 2023. Prediction of hardness of mild steel welded joints in a tungsten inert gas welding process using artificial neural network. *JASEM*, 27(11), pp.2381-2386.
- Otimeyin, A. W., Achebo, J. I., and Frank, U. (2025). Advanced Modelling and Optimization of Weldment Responses Using Statistical and Metaheuristic Techniques. *American Journal of Mechanical and Materials Engineering*, 9 (1), 25-36. <https://doi.org/10.11648/j.ajmme.20250901.13>